A New QM/MM Method Oriented to the Study of Ionic Liquids

M. Luz Sánchez,[a] José C. Corchado,[a] M. Elena Martín,[a] Ignacio Fdez. Galván,[b] Rute Barata-Morgado,[a] and Manuel A. Aguilar*[a]

The interest on room temperature ionic liquids has grown in the last decades because of their use as all-purpose solvent and their low environmental impact. In the present work, a new theoretical procedure is developed to study pure ionic liquids within the framework of the quantum mechanics/molecular mechanics method. Each type of ion (cation or anion) is considered as an independent entity quantum mechanically described that follows a differentiated path in the liquid. The method permits, through an iterative procedure, the full coupling between the polarized charge distribution of the ions and the liquid structure around them. The procedure has been tested with 1-ethyl-3-methylimidazolium tetrafluoroborate. It was found that, similar to non-polar liquids and as a consequence of the low value of the reaction field, the cation and anion charge distributions are hardly polarized by the rest of molecules in the liquid. Their structure is characterized by an alternance between anion and cation shells as evidenced by the coincidence of the first maximum of the anion–anion and cation–cation radial distribution functions with the first minimum of the anion-cation. Some degree of stacking between the cations is also found. © 2015 Wiley Periodicals, Inc.

DOI: 10.1002/jcc.24023

Introduction

Over the last decades, a huge research effort has been directed toward the searching for alternative solvents. For instance, there is an increasing interest in green solvents, that is, solvents that minimize the environmental impact resulting from their use in chemical production, or electrical conducting solvents, mainly in relation with their use in electric battery applications. Room temperature ionic liquids (RTIL) constitute a good alternative to traditional acid and organic solvents as they are electrically conducting fluids, not volatile, they melt without decomposing or vaporizing below 100 °C or even at room temperature and they dissolve many different types of compounds.[1,2] One characteristic of RTILs that accounts for their properties is that their ions are poorly coordinated. The ions in a RTIL are, in general, big and nonsymmetrical, the irregular shapes reduce the ionic attractions and that prevents the ions packing together neatly. So in the structure of RTILs, it is possible to find individual ions and short-lived ion pairs. Besides, as they are composed of at least two components, cation and anion, different combinations of them permit to design a tremendous variety of solvents. Through a proper choice of each one of their ions, a solvent can be designed for a particular use or for a specific task.

As a consequence of this interest many research groups have studied and reported the physical properties, the structure, and dynamics of this kind of liquids.[3–5] An important point to elucidate is how the molecular and electronic structures of the ions determine the macroscopic properties of the liquid. Ionic liquids are made from molecular ions that display spatially extended charge distributions, which affect to their mutual interactions and consequently, to their spatial distribution.

The theoretical study of ionic liquids is complicated because of the difficulties inherent to the study of liquids, that is, the lack of symmetry and the existence of a manifold of configurations thermally accessible that must be included to obtain statistically significant results, one must add the complications associated to the long-range nature of the electrostatic interactions and the possible presence of specific interactions between nonsymmetric charged molecules.[6] *Ab initio* molecular dynamics and Car–Parrinello methods are very precise techniques that permit to obtain information on the relationship between the electron distribution and the ionic spatial structure. They have been applied to the study of different RTILs.[7–10] Unfortunately, these are very intensive computational procedures and their use is, in general, restricted to small model systems, around some tens of ions, something that is not in keeping with the long-range nature of the interactions that characterize RTILs. Classical molecular dynamics simulations have been the method preferred for several research groups[11,12] and many of the RTILs properties have been obtained and compared with experimental data; however, this method does not provide a detailed description of the electronic structure of the ions and it accounts for the mutual polarization of the ions only in an implicit way. Between both strategies quantum mechanics/molecular

[a] M. L. Sánchez, J. C. Corchado, M. E. Martín, R. Barata-Morgado, M. A. Aguilar
Área de Química Física, University of Extremadura, Avda. Elvas s/n, Edif. José M[a] Vigera Lobo 3[a], planta Badajoz, 06006, Spain
E-mail: maguilar@unex.es
[b] I. Fdez. Galván
Department of Chemistry–Ångström, The Theoretical Chemistry Programme, Uppsala University, PO Box 518, SE-751 20 Uppsala, Sweden

mechanics (QM/MM) methods seem to be a good choice. However, their application to the study of ionic liquids is not free of problems. As it is well-known, in this kind of methods, a part of the system is described using QM while the rest is represented through a classical force field. When applied to the study of molecular liquids the selection of the QM part does not pose problems, it includes only one molecule representative of the liquid. However, in ionic liquids nothing similar to a "molecule" can be defined. Each type of ion (cation or anion) must be considered as an independent entity that follows a differentiated path in the liquid. So, we face a problem where it is necessary to define two QM subsystems (the anion and the cation) that interact mutually and with the rest of the system. In the next section, a new QM/MM method designed for the study of ionic liquids is presented. Then, in Computational Details section, the method is tested with the 1-ethyl-3-methylimidazolium tetrafluoroborate (emim-BF4). The main conclusions are summarized in the last section.

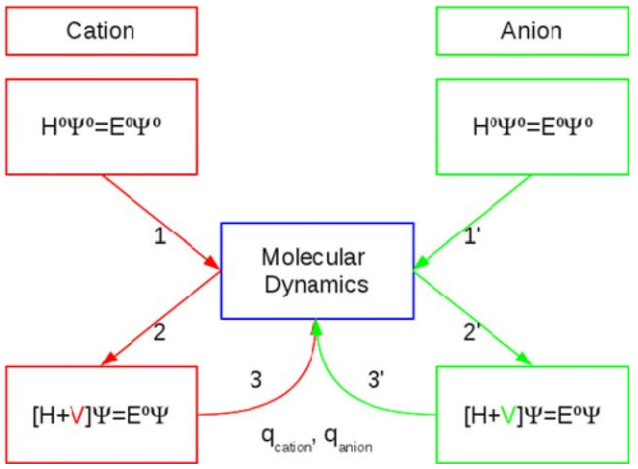

Scheme 1. The basic scheme of the new procedure with the ASEP/MD method. [Color figure can be viewed in the online issue, which is available at wileyonlinelibrary.com.]

Methodology

The main aim of this work is to put forward a new QM/MM method designed for studying ionic liquids. The method makes use of the mean field approximation (MFA), and it is related to the average solvent electrostatic potential/molecular dynamics (ASEP/MD) methodology[13–17] developed in our group for the study of solvent effects in molecular liquids. The main characteristics of the method are: (1) in optimizing the geometry and electronic structure of the ions, we keep fixed the liquid structure. In the same way, when the liquid phase space is explored it is assumed that the geometry and charge distribution of the ions do not change. Ion wave-functions and the liquid structure around them are optimized using an iterative procedure. (2) The perturbation generated by the liquid on the ions enters into the ion Hamiltonian in an averaged way. (3) The charge distribution of the ions obtained from the QM calculation are used to update the force field of all the molecules (quantum and classical) in the MD simulation. (4) The solute optimization is performed using the free energy gradient method.

Before describing the procedure, it is important to clarify the way in which the total system is split into its quantum and classical parts. We consider two quantum systems: one cation and one anion, randomly chosen between the ions of the RTIL. However, they are not described quantum mechanically simultaneously. When the cation is quantum mechanically described the anion is classically represented and vice versa. The rest of the cations and anions of the ionic liquids are always described classically.

Scheme 1 can help to clarify the different steps of the procedure. (1) It starts by performing two *in vacuo* quantum calculations, one for the cation and another one for the anion; from these, we get two sets of electrostatic-potential-fitted (ESP) charges for them. (2) These ESP charges are used during the MD simulation for representing all the cations and anions included in the simulation box. During the MD calculations both the geometry and charge distribution for the anions and cations are kept fixed. (3) Then, a cation (anion) is randomly chosen and the ASEP generated by the liquid in the cation (anion) position is calculated. (4) This potential is introduced into the cation (anion) Hamiltonian as a perturbation. Obviously, the ASEP is different for the cation and the anion as they have different ionic environments. By solving the corresponding Schrödinger equations for the cation and the anion, we get the wavefunctions and properties for the cation and anion but now polarized by the environment. From this information, one can get a new set of ESP charges that can be introduce into the MD calculation, step 2. Note that, as indicated before, these ESP charges are used to update the charge distribution of all the ions of the liquid. Obviously the charge distribution of each cation (anion) depends on its particular surroundings, but given that we are using a mean field theory, we can consider that the average electric field that each cation (anion) feels is the same for all of them, and hence we can suppose that all the cations (anions) in the liquid have identical average charge distributions. This means that we can use the charge distribution obtained for the cation (anion) quantum mechanically treated to represent all the cations (anions) in the MD calculation. The procedure continues until the energies and charges of the cation and anion converge. As the QM calculation and the MD simulation are consecutive the method can be easily parallelized. It is enough to use the parallelized (if available) versions of the external programs. The calculation of the ASEP can also be easily parallelized once the system configurations are known.

We pass to detail the proposed methodology.

Let us suppose the total system is formed by N anions and N cations in a volume V. As usual in QM/MM methods, the total Hamiltonian of the system is defined as:

$$\hat{H} = \hat{H}_{QM} + \hat{H}_{class} + \hat{H}_{int} \quad (1)$$

corresponding to the quantum region, $\hat{H}_{QM}$, the classical region, $\hat{H}_{class}$, and the interaction between them, $\hat{H}_{int}$. The quantum region is formed by a randomly chosen anion (or

cation). The classical region is formed by the remaining $N-1$ anions and N cations (or $N-1$ cations and N anions). This distinction is relevant only during the quantum calculation as in the MD simulation all the ions are treated classically.

The energies and wavefunctions of the QM regions are obtained by solving the effective Schrödinger equation:

$$\left(\hat{H}_{\mathrm{QM}}+\langle\hat{H}_{\mathrm{int}}\rangle\right)|\Psi\rangle=\bar{E}|\Psi\rangle \tag{2}$$

Here, the mean field interaction Hamiltonian, $\langle\hat{H}_{int}\rangle$, is defined as[13,18,19]:

$$\langle\hat{H}_{\mathrm{int}}\rangle=\int dr\cdot\hat{\rho}\cdot\langle V_{\mathrm{s}}(r)\rangle \tag{3}$$

where $\hat{\rho}$ is the charge density operator of the QM region (the ion) and $\langle V_{\mathrm{s}}(r)\rangle$, which is named ASEP, is the average electrostatic potential generated by the classical region at the position r. The brackets denote a statistical average over the configurational space of the classical subsystem. Note that the information necessary to calculate $\langle V_{\mathrm{s}}\rangle$ is obtained from a classical molecular dynamics simulation.

From a computational point of view, it is convenient to split the interaction term into two components associated to the electrostatic and van der Waals contributions:

$$\hat{H}_{\mathrm{int}}=\hat{H}_{\mathrm{int}}^{\mathrm{elect}}+\hat{H}_{\mathrm{int}}^{\mathrm{vdW}} \tag{4}$$

In general, it is assumed that $\hat{H}_{\mathrm{int}}^{\mathrm{vdW}}$ has a small effect on the solute wavefunction, and therefore, it is usual to represent it through a classical potential that depends only on the nuclear coordinates but not on the electron coordinates. If this is the case, and for a given configuration of the classical subsystem, the $\hat{H}_{\mathrm{int}}^{\mathrm{vdW}}$ term can be simply added to the final value of the energy as a constant.

Until now, we have shown how the classical region perturbs the quantum one; however, the classical subsystem structure depends, self consistently, on the charge distribution of the quantum subsystem, that is, $\langle V_{\mathrm{s}}\rangle\equiv\langle V_{\mathrm{s}}(\Psi)\rangle$. As a consequence, eq. (2) becomes an implicit nonlinear expression: the wavefunction depends on the ASEP which, in turn, depends on the wavefunction. A consequence of the non-linearity of eq. (2) is that it needs to be solved iteratively.

In our model, the ASEP is represented and introduced into the Hamiltonian as a set of point charges. To keep a tractable number of charges only those charges associated to ions that belong to the first solvation shell are include explicitly. The effect of the remaining solvent molecules is described through potential-fitted charges. This permits to reduce the number of charges to only a few thousands. More details about the calculation and representation of the ASEP can be found elsewhere.[13–17]

In optimizing the geometry of the quantum systems, we use a variant of the free energy gradient method[20–22] that permits the determination of critical points on free energy surfaces (FES). The FES is defined as the energy associated with the time average of the forces acting on the molecular ion. Let A be the Helmholtz free energy of a system. The force on the FES (the force felt by the quantum subsystem) is

$$\langle F(R)\rangle=-\frac{\partial A}{\partial R}=-\left\langle\frac{\partial E}{\partial R}\right\rangle=-\frac{\partial E_{\mathrm{QM}}}{\partial R}-\left\langle\frac{\partial E_{\mathrm{int}}}{\partial R}\right\rangle \tag{5}$$

R beinthe nuclear coordinates of the quantum ion, E the energy obtained as the solution of the Schrödinger equation (1), $E_{\mathrm{QM}}=\langle\Psi|\hat{H}_{\mathrm{QM}}|\Psi\rangle$, $E_{\mathrm{int}}=\langle\Psi|\hat{H}_{\mathrm{int}}|\Psi\rangle$ and where we have assumed that E_{class} does not explicitly depend on the solute nuclear coordinates R and that the geometry of the quantum part is kept fixed during the MD simulation. The brackets denote a configurational average. Note that E incorporates both intramolecular, E_{QM}, and intermolecular, E_{int}, contributions.

In the same way, the Hessian reads:

$$\langle H(R,R')\rangle=\left\langle\frac{\partial^2E}{\partial R\partial R'}\right\rangle-\beta\left\langle\frac{\partial E}{\partial R}\left(\frac{\partial E}{\partial R'}\right)^{\mathrm{T}}\right\rangle+\beta\left\langle\frac{\partial E}{\partial R}\right\rangle\left\langle\frac{\partial E}{\partial R'}\right\rangle^{\mathrm{T}} \tag{6}$$

where the superscript T stands for transpose and $\beta=1/k_{\mathrm{B}}T$. The last two terms in eq. (6) are related to the thermal fluctuations of the force.

As for the energy, it is convenient to split the interaction term into two components associated with the electrostatic and van der Waals contributions:

$$\langle F(R)\rangle=-\frac{\partial E_{\mathrm{QM}}}{\partial R}-\left\langle\frac{\partial E_{\mathrm{int}}^{\mathrm{elect}}}{\partial R}\right\rangle-\left\langle\frac{\partial E_{\mathrm{int}}^{\mathrm{vdW}}}{\partial R}\right\rangle \tag{7}$$

At this point one can introduce the MFA by replacing the average derivative of $E_{\mathrm{int}}^{\mathrm{elect}}$ with the derivative of the average value. The force now reads[23]:

$$\langle F(R)\rangle=-\frac{\partial E_{\mathrm{QM}}}{\partial R}-\frac{\partial-E_{\mathrm{int}}^{\mathrm{elect}}}{\partial R}-\left\langle\frac{\partial E_{\mathrm{int}}^{\mathrm{vdW}}}{\partial R}\right\rangle \tag{8}$$

and, analogously, the Hessian reads:

$$\langle H(R,R')\rangle=-\frac{\partial^2E_{\mathrm{QM}}}{\partial R\partial R'}-\frac{\partial^2\bar{E}_{\mathrm{int}}^{\mathrm{elect}}}{\partial R\partial R'}-\left\langle\frac{\partial^2E_{\mathrm{int}}^{\mathrm{vdW}}}{\partial R\partial R'}\right\rangle \tag{9}$$

where, according to the MFA, the force fluctuation term has been neglected. Once the gradient and Hessian values are known, we can use any of the usual optimization methods to get the optimized geometry incorporating the optimization step into Scheme 1. In the present work, the rational function method[24] was used.

Computational Details

The proposed methodology has been applied to the study of the emim-BF4 ionic liquid, see Figure 1. During the QM/MM iterative process, the programs used were: Gaussian 98[25] for the QM calculations and Moldy[26] for the MD simulations.

Full ground state geometry optimizations for the cation and anion using Density Functional Theory (DFT) were performed allowing the total relaxation of all the degrees of freedom. The DFT calculations were carried out with the B3LYP[27] functional and with a 6-31G* basis set. Previously, we checked that the

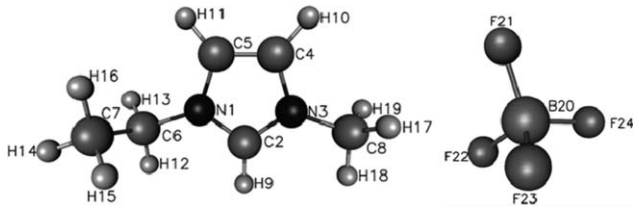

Figure 1. 1-ethyl-3-methylimidazolium-BF4: Atom numbering.

use of larger basis sets including diffuse functions do not modify the charge distribution of the ions.

The force field was constructed by combining Lennard-Jones interatomic interactions taken from Liu et al.[28] with electrostatic interactions. We assume fixed geometry during the MD simulations, so no intramolecular parameters were necessary. The system was composed of 130 cations and 130 anions. The atomic charges of the ions were obtained from DFT/6-31G* calculations using the Charges from Electrostatic Potential, Grid method.[29] The charges of all the ions were updated at each ASEP/MD cycle. Periodic boundary conditions were applied. The long-range electrostatic interaction was calculated with the Ewald method.[30] The temperature was fixed at 303.15 K and 363.15 K using the Nosé–Hoover thermostat[31] and the equilibrium densities were 1.24 g/cm^3 and 1.197 g/cm^3, respectively. Each simulation was run for 150,000 time steps, where 50,000 were for equilibration and 100,000 for production. A time step of 0.5 fs was used. Final results were obtained by averaging the last five ASEP/MD cycles, so, they include information of 250 ps. To check that the sluggish nature of ionic liquids does not introduce bias or artifacts in the results, calculations were repeated using different initial configurations, different seeds, and choosing different molecules as quantum part of the system. The new initial configurations were generated by decreasing the charge on each ion and, at the same time, increasing the temperature. Then, the charge and temperature initial values were reestablished. In all cases, similar values for the charge distributions, energies, radial distribution functions (rdf), and so forth were found.

Results

In this section, we apply the above developed methodology to the study of the emim-BF4 ionic liquid. To highlight the characteristics of ionic liquids, we will compare the results for emim-BF4 with those obtained from molecular polar liquids. All the calculations were performed at two temperatures 303.15 K and 363.15 K. The results at both temperatures are almost the same; by simplicity, only the 363.15 K data will be discussed.

Polarization

We start by analyzing the charge distribution of the ions and their evolution along the self-consistent process, see Table 1. The values at cycle 0 correspond to the isolated cation (or anion). The anion has a very symmetrical charge distribution where the negative charge is carried by fluorine atoms. On the contrary, the emim cation has a more complex charge distribution where the positive charge spreads out over the whole molecule. The larger charges are on the hydrogen atoms bonded to the ring and the methyl group. It is worth noting that the cation and anion charge distributions are hardly modified when one passes from the isolated ion (cycle 0) to the liquid phase. As a consequence, the iterative procedure converges in only 2–3 cycles. This behavior differs from that shown by molecular polar liquids where there exists a strong polarization of the molecule and where at least 5–10 ASEP/MD cycles are necessary to reach convergence and it is a consequence of the small value of the electric field generated by the rest of the ions of the RTIL in the volume occupied by the QM ion. On the contrary, in polar molecular liquids the electric field is, in general, large. Obviously, the electrostatic interaction energy (and hence the electrostatic potential) between the ions is very large. However, the potential is very homogeneous inside the ion's volume, and its gradient (the electric field) is close to cero. This conclusion is valid both for the cation and anion despite the differences in the symmetry of their charge distributions. Polar liquids, on the contrary, display much smaller values of the interaction energy but a larger potential asymmetry, and hence, they suffer larger polarizations of the their charge distributions. Consequently, while in polar molecular liquids it is a bad strategy to use gas phase charges in MD calculations this approximation works well in emim-BF4.

Because of the separation between quantum and classical subsystems, QM/MM methods do not account for the charge

Table 1. Summed atomic charges (in *e*) and standard deviation on different groups of the emim cation.

		Cycle							
		0	1	2	3	4	5	Average	Std. dev.
Ring		0.517	0.543	0.546	0.543	0.544	0.545	0.544	0.001
	N1	0.056	0.045	0.042	0.038	0.041	0.045	0.042	0.003
	C2	−0.082	−0.074	−0.086	−0.083	−0.084	−0.085	−0.082	0.005
	N3	0.156	0.198	0.197	0.197	0.198	0.196	0.197	0.001
	C4	−0.119	−0.159	−0.154	−0.156	−0.160	−0.159	−0.158	0.002
	C5	−0.126	−0.148	−0.150	−0.149	−0.148	−0.149	−0.149	0.001
	H9	0.218	0.248	0.259	0.259	0.259	0.258	0.256	0.005
	H10	0.201	0.211	0.212	0.212	0.212	0.211	0.211	0.000
	H11	0.213	0.223	0.226	0.225	0.226	0.227	0.226	0.001
CH_2	(Ethyl)	0.210	0.244	0.243	0.246	0.245	0.242	0.244	0.001
CH_3	(Ethyl)	0.073	0.034	0.033	0.033	0.035	0.035	0.034	0.001
CH_3	(Methyl)	0.156	0.179	0.178	0.178	0.177	0.179	0.178	0.001

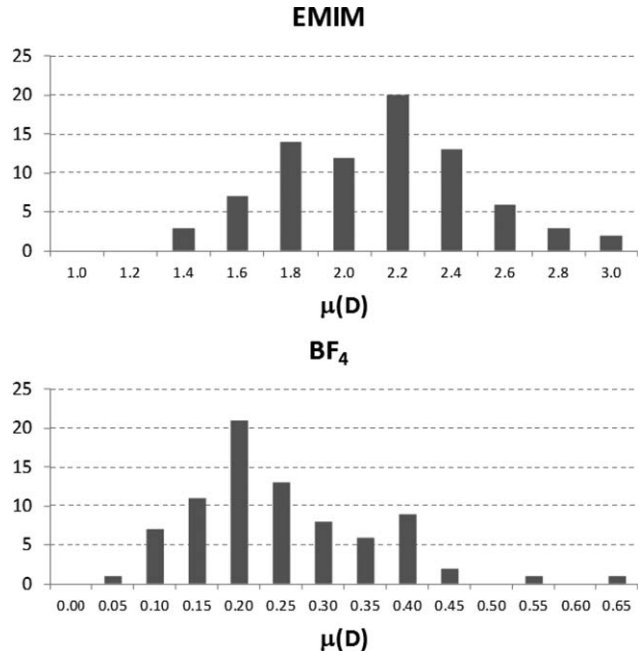

Figure 2. Dipole moment histogram a) emin, b) BF4.

transfer between the ions. To check the effect of the charge transfer on the ions charge distribution, 80 randomly chosen configurations were selected. For each configuration, a quantum calculation was performed, including the cation and an anion of the first solvation shell. For each one of the 80 configurations, the cation–anion charge transfer was analyzed. The results point out that the averaged charge transfer between the ions is very small, less than 0.03 *e*, with a standard deviation of 0.007. This value is so small that its effect on the cation–anion electrostatic interaction is negligible (lower than 0.1 kcal/mol). Therefore, the separation quantum ion-classical environment is justified and a QM/MM methodology seems to be adequate in studying this kind of system. Our results depart from those obtained by other authors that found charge transfer values close to 0.3 *e* using chloride as anion. To check the origin of this discrepancy, several calculations were performed. First, an ionic pair was studied using fluoride as anion, a charge transfer of about 0.3 *e* was found, similar to the result provided by chloride. Next, the emim-BF4 ionic pair in gas phase was studied. In this case, a charge of 0.06 *e* is transferred between the ions. This value is very similar to that found in solution. Finally, clusters of several sizes (1 cation + 5 anion, 1 cation + 8 anions, 7 cations + 8 anions, 12 cations + 8 anions) were considered. The charges transferred from the emim cation were 0.09, 0.1, 0.05, and 0.06 *e*, respectively. In all cases, the charge is lower than 0.1 *e*. Furthermore, the consideration of the remaining ions in the liquid does no modify the results. So our discrepancy with previous results seems to be related with the nature of the anion: fluoride or chloride anions provide charge transfer values close to 0.3 *e* while BF4 yields charge transfer lower than 0.1 *e*. These values confirm the conclusions from a previous study of Choi et al.[32] using symmetry-adapted perturbation theory, which found no substantial contribution from the charge transfer component in the liquid.

Previous Car–Parrinello calculations[10] have highlighted the importance of charge fluctuations in RTILs. Using the same set of 80 quantum calculations indicated above, we have analyzed the charge and dipole fluctuations of the ions. Obviously, in the case of ions the absolute value of the dipole moment depends on the origin of the coordinate axes and only its variations have physical sense. A histogram with the dipole values is displayed in Figure 2. The charges and dipole moment of the cation fluctuate in about a 34%, this value being somewhat lower than that proposed by Krekeler et al.[10] for the dimethyl derivative, where fluctuations were estimated in about 50%. The average value of the dipole moment obtained from the 80 quantum calculations (2.02 D) agreed with the ASEP/MD value (2.09 D). The difference between the two dipoles is lower than 5%. Similar values were found for the anion (0.23 D vs. 0.10 D). It can be concluded that, in this system, the MFA works very well.

Structure

Here, we consider both the internal geometry of the ions and the spatial structure of the RTIL. Regarding the internal geometries of the anion and cation, see Table 2, the bond lengths display only small variations (lower than 0.01 Å) when they pass from isolated to associated in the liquid. A similar trend is found in bond and dihedral angles with variations lower than 1°. These small geometry perturbations are a consequence of the

Table 2. Geometric parameters, bond (in Å) and angles (in degrees) in gas phase and in liquid of the emim cation.

	Gas	Cycle 1	Cycle 2	Cycle 3	Cycle 4	Average	Std. dev.
N1-C2	1.338	1.330	1.337	1.337	1.337	1.336	0.003
C2-N3	1.339	1.331	1.337	1.337	1.337	1.335	0.003
N3-C4	1.383	1.375	1.383	1.383	1.383	1.381	0.004
C4-C5	1.363	1.358	1.362	1.362	1.362	1.361	0.002
C5-N1	1.383	1.374	1.383	1.383	1.383	1.381	0.005
N1-C6	1.483	1.477	1.476	1.477	1.477	1.477	0.000
C6-C7	1.527	1.524	1.525	1.524	1.524	1.524	0.000
N3-C8	1.470	1.464	1.466	1.465	1.465	1.465	0.001
C2-H9	1.080	1.062	1.081	1.081	1.081	1.076	0.009
C4-H10	1.079	1.067	1.077	1.078	1.078	1.075	0.005
C5-H11	1.079	1.063	1.076	1.078	1.078	1.074	0.007

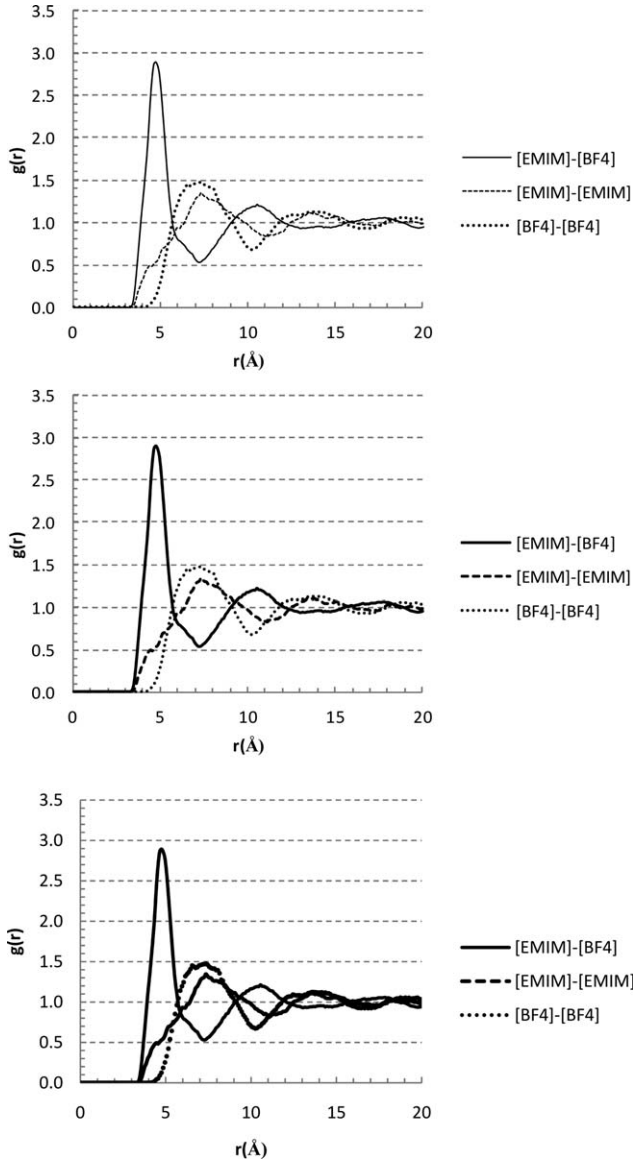

Figure 3. Cation–anion, cation–cation, and anion–anion radial distribution functions.

small values of the electric field generated by the liquid in the volume occupied by the ions. Unlike dipole moment values, bond length and angle fluctuations are very small.

As for the liquid structure, we analyze several pair rdf. Figure 3 displays the cation–anion, cation–cation and anion–anion rdfs. In the cation–anion rdf, there is a well-defined peak at 5.0 Å, with a coordination number of 6.5. This value agrees with the reported crystal structure data for dmim-Cl,[1] where it was found that each cation interacts with six anions. There are also peaks corresponding to the second and third coordination shells at 10 Å and 17.5 Å, respectively. The first maximum of the anion–anion and cation–cation rdf agree with the first minimum of the anion-cation rdf and it evidences a structure where anion and cation shells alternate, a fact that is confirmed by Figures 4a and 4b, which display the three-dimensional distribution of center of mass of BF4 around emim and emim around BF_4, respectively. The volumes with larger probability of finding the anions are close to the three hydrogen atoms of the ring.

To determine whether hydrogen bonds are present or not in the liquid, we have analyzed some atom–atom rdfs. Probably the most interesting are the F(BF4)-H(emin) rdfs. Figure 5a displays the rdfs corresponding to the hydrogen atoms bonded to the carbon atoms of the imidazolium ring. The structure is characteristic of a hydrogen bond. Note, that these hydrogen atoms support a positive charge (about $+0.2$ *e*) while the fluorine atoms of the anion have a negative charge (-0.4 *e*). The first peak in the rdf appears at 2.2 Å for the hydrogen bonded to C2 and at 2.5 Å for the hydrogen atoms bonded to C4 and C5. These values are similar to those obtained from X-ray diffraction studies of emim-BF4 crystal structures. So Matsumoto et al.[33] find hydrogen bond

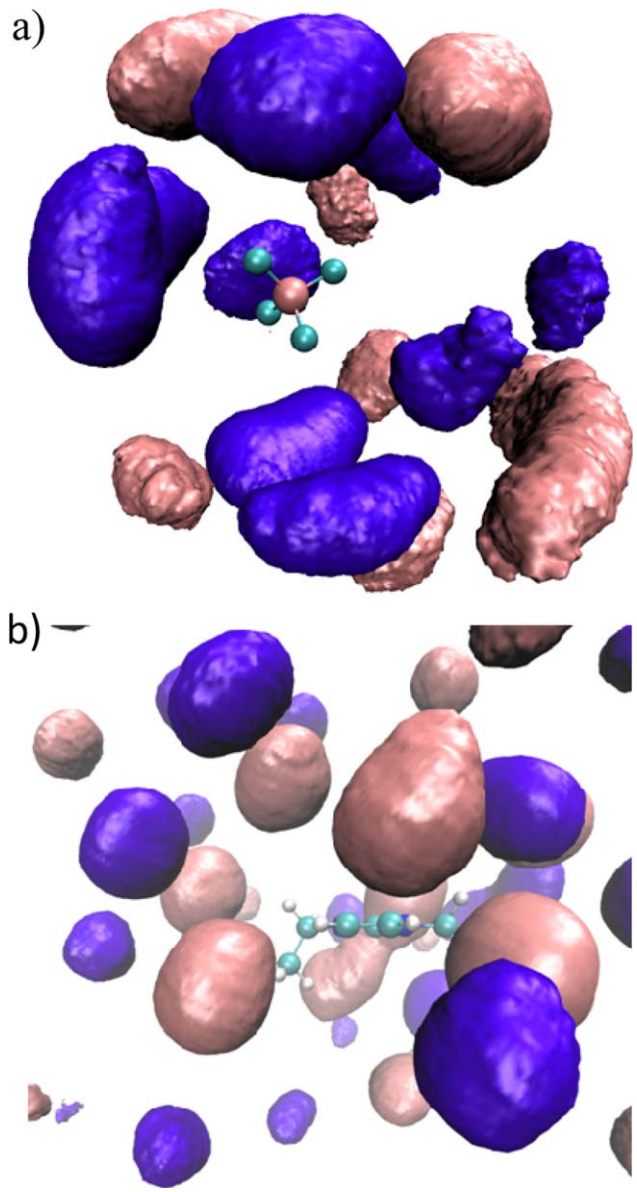

Figure 4. a) Three-dimensional probability distribution around BF4 and b) three-dimensional probability distribution around emin. Blue: emim, brown: BF4.

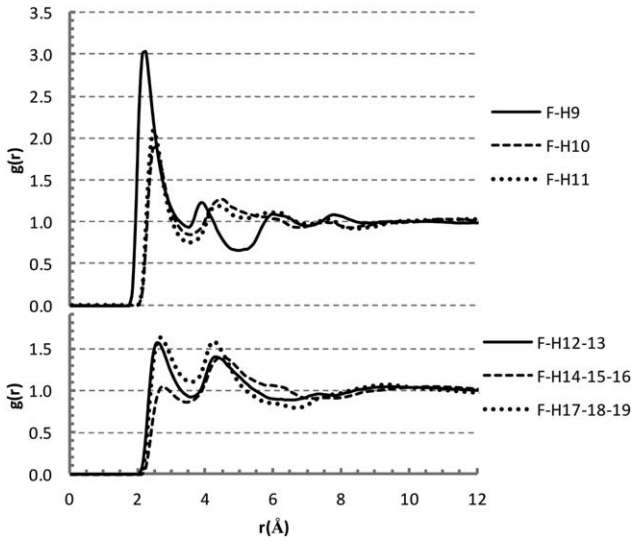

Figure 5. Fluorine (BF4)-hydrogen (emin) radial distribution functions (Å).

distances of 2.25 Å and 2.36 Å, respectively. The differences between liquid and crystal HB angles are somewhat larger. So, ASEP/MD yields to a C—H—F angle value of about 120°, while in the crystal this angle takes a value of 154.6°. These diffrences are related to the different reaglement of ions in the crystal and the liquid. The hydrogen bonds above mentionated can be classified as weak attending to geometrical criteria. Our data corroborate the results of Johnson et al.[33] that studying cryogenic ion spectroscopy propose who the observed bulk red shift of the C2—H band is too small (<10 cm^{-1}) for hydrogen bonding to be a dominant structural feature. There are also a well-defined feature in Figure 5b corresponding to the rdf between fluorine atoms and the hydrogen atoms of the methyl and ethyl groups. In all the cases, the height of the first peak correlates with the charged supported by the hydrogen atoms.

The possible stacking between the imidazolium rings was also considered. Some X-ray studies[34,35] have found face–face stacking in RTIL; however, neutron diffraction studies have not confirmed this. Figure 6 displays the numerical density of H9 and N1 and N2 atoms of emim around the imidazolium ring. Cations below and above the imidazolium ring tend to be

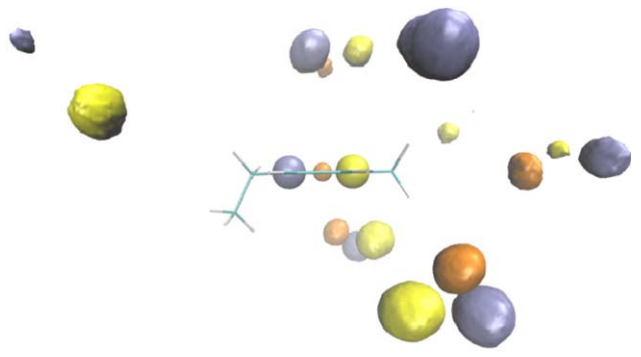

Figure 6. Three-dimensional probability distribution showing the presence of stacking. Color code: N3-yellow, N1-blue, H9-orange.

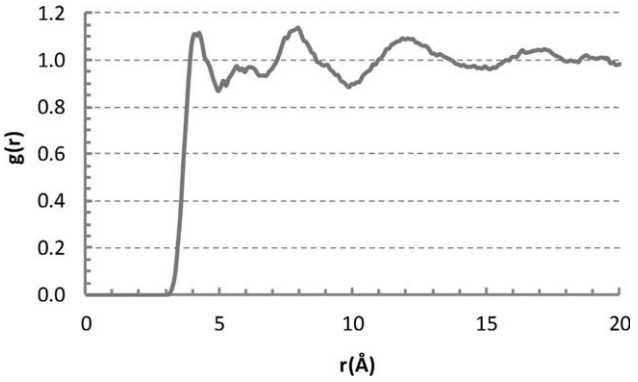

Figure 7. Ethyl-ethyl radial distribution function.

placed preferentially with the rings nearly parallel. Our results seem to confirm the X-ray results. However, there are also other emim–emim pairs where the orientation is almost perpendicular. In any case, the liquid structure is different from crystal structure where emim cations adopt a pillar-like stacking.[34]

Finally, the possible existence of tail aggregation was also investigated. This structural characteristic has been found[36] in some alkyl-methyl imidazolium cations. In these systems, the alkyl group points to the center of the imidazolium ring and can be characterized by the presence of a large peak in the alkyl-gravity center rdf, see Figure 7. Unlike other related systems, emim displays a very small tail aggregation, probably due to the short length of the alkyl chain.

Energies

Tables 3 and 4 display the interaction energies between the cation (anion) and the rest of the liquid. The contribution of different parts of the ions to the total energy was also analyzed. As corresponds to charged systems, the interaction energy between the cation (anion) and the environment is large, −95.5 kcal/mol for the cation and −71.86 kcal/mol for the anion. As expected, the larger contribution comes from the electrostatic component, the contribution of the solute

Table 3. Ion-solvent interaction energies and standard deviation, in kcal/mol.

		Electrost.	vdW	Total
BF4	Cycle 1	−66.5	−5.9	−72.4
	Cycle 2	−62.5	−5.8	−68.3
	Cycle 3	−70.3	−5.9	−76.2
	Cycle 4	−68.3	−6.0	−74.3
	Average	−66.9	−5.9	−72.8
	Std. dev.	3.3	0.07	3.4
EMIM				
	Cycle 1	−76.8	−6.5	−83.3
	Cycle 1	−82.1	−19.0	−101.1
	Cycle 2	−79.4	−19.3	−98.7
	Cycle 3	−75.2	−19.4	−94.6
	Cycle 4	−80.2	−19.4	−99.6
	Average	−79.2	−19.3	−98.5
	Std. dev.	2.9	0.2	2.8

Table 4. Group contribution to the emim-solvent electrostatic interaction energy and standard deviation, in kcal/mol.

		⟨E⟩	Std. dev.
Ring		−46.1	1.5
	N1	−3.2	0.2
	C2	6.8	0.4
	N3	−15.1	0.4
	C4	11.2	0.3
	C5	10.5	0.4
	H9	−24.7	0.8
	H10	−15.1	0.5
	H11	−16.5	0.5
CH_2	(Ethyl)	−17.6	0.5
CH_3	(Ethyl)	−1.7	0.1
CH_3	(Methyl)	−13.2	0.6
Total		−78.6	2.7

polarization component is negligible while the van der Waals contribution represents about 20% for the cation but only 8% for the anion. To analyze the group contributions to the interaction energy, we have split the cation in four parts: the ring and the three methyl or methylene groups. In the case of the ring, we also consider the contribution of each atom. Because of its symmetry, in the anion this analysis has a lower interest. In the cation, the main contribution (about 58%) comes from the ring. C6 and C8 groups have similar contribution while the contribution of C7 group is completely negligible. This result confirms the absence of tail aggregation in this system. Regarding the ring atoms contributions and in agreement with the hydrogen bond lengths and rdf results, see Figure 5, the larger contribution comes from H9. Because of the symmetry of the cation, the H10 and H11 contributions are very similar. However, there are significant differences in the behavior of N1 and N3: the interaction energy of N3, bonded to the methyl group, is considerable larger than the interaction energy of N1, bonded to the ethyl group. This difference is probably related to the different charges of the nitrogen atoms, which in turn are related to the different inductive effect of methyl and ethyl groups.

Finally, we have analyzed solvent effects on some reactivity indices as are chemical potential, $\mu = \frac{1}{2}(\varepsilon_{HOMO} + \varepsilon_{LUMO})$, and chemical hardness, $\eta = \varepsilon_{HOMO} - \varepsilon_{LUMO}$, see Table 5. The electrostatic potential generated by the liquid produces a homogeneous and systematic energy shift of the HOMO and LUMO orbitals. In fact, the chemical hardness is the same in gas phase and inside the liquid. On the contrary, the absolute value of the chemical potential decreases in both the cation and the anion (note that the electrostatic potential generated by the liquid is negative on the cation but positive on the anion).

Table 5. Calculated reactivity indices (in a.u.) in gas phase and in the liquid.

		HOMO	LUMO	Hardness	Chem. pot.
EMIM	Gas	−0.432	−0.180	0.251	−0.306
	Liquid	−0.315	−0.060	0.255	−0.188
	Shift	0.116	0.120	0.004	0.118
BF4					
	Gas	−0.115	0.458	0.574	0.1717
	Liquid	−0.222	0.350	0.573	0.0639
	Shift	−0.107	−0.108	−0.001	−0.108

Conclusions

A new QM/MM method oriented to the study of ionic liquids has been introduced. The method permits, through an iterative procedure, the full coupling between the polarized charge distribution of the ions and the liquid structure around them. At each cycle, the geometry and charge distribution of all the ions that form the liquid are updated. A main conclusion of our research is that in emim-BF4 the average polarization of the ions is very small. Average charge distributions of the ions inside the liquid are very similar to those of the isolated ions. This fact is related with the low value of the reaction electric field generated by the liquid. Furthermore, the charge transfer between ions is also negligible. Although the dipole fluctuations can be important, the MFA provides an adequate description of the average charge distribution.

From the analysis of the rdfs, it becomes clear that the liquid structure is characteristic of ionic systems where cation and anion shells alternate. There is some degree of stacking in the cation, but in the molecular plane the structure is determined by the presence of weak hydrogen bonds between the hydrogen atoms of the imidazolium ring and the fluorine atoms of the anion. Small differences in the atomic charges between the hydrogen atoms translate in differences in the strength of the hydrogen bonds: hydrogen atoms bonded to C2 form stronger bonds than hydrogen atoms bonded to C4 and C5.

Keywords: solvent effects · quantum mechanic/molecular mechanic · average solvent electrostatic potential/molecular dynamics · room temperature ionic liquids

How to cite this article: M. Luz Sánchez, J. C. Corchado, M. Elena Martín, I. Fdez. Galván, R. Barata-Morgado, M. A. Aguilar. *J. Comput. Chem.* **2015**, *36*, 1893–1901. DOI: 10.1002/jcc.24023

[1] C. Hardacre, J. D. Holbrey, M .Nieuwenhuyzen, T. G. A. Youngs, *Acc. Chem. Res*. **2007**, *40*, 1146.
[2] P. Wasserscheid, T. Welton, Eds. Ionic Liquids in Systehesis; VCH Verlag: Weinheim, Germany, **2003**
[3] S. Takahashi, N. Koura, M. Murase, H. Ohno, *J. Chem. Soc., Faraday Trans*. II **1986**, *82*, 49.
[4] S. Takahashi, K. Suzuya, S. Kohara, N. Koura, L. A.Curtiss, M.-L Saboungi, Z. *Phys. Chem*. **1999**, *209*, 209.
[5] K. Matsumoto, R. Hagiwara, Y. Ito, S. Kohara, K. Suzuya, *Nucl. Instrum. Methods Phys. Res. B* **2003**, *199*, 29.
[6] R. M. Lynden-Bell, M. G. Del Pópolo, T. G. A. Youngs, J. Kohanoff, C. G. Hanke, J. B. Harper, C. C. Pinilla, *Acc. Chem. Res*. **2007**, *40*, 1138.
[7] Z. Meng, A. Dolle, W. R. Carper, *THEOCHEM J. Mol. Struct*. **2002**, *585*, 119.
[8] Y. U. Paulechka, G. J. Kabo, A. V. Blokhin, O. A. Vydrov, J. W. Magee, M. Frenkel, *J. Chem. Eng. Data* **2003**, *48*, 457.
[9] E. A. Turner, C. C. Pye, R. D. Singer, *J. Phys. Chem. A* **2003**, *107*, 2277.

[10] C. Krekeler, F. Dommert, J. Schmidt, Y. Y. Zhao, C. Holm, R. Berger, L. D. Site, *Phys. Chem. Chem. Phys*. **2010**, *12*, 1817.
[11] C. G. Hanke, S. L. Price, R. M. Lynden-Bell, *Mol. Phys*. **2001**, *99*, 801.
[12] C. J. Margulis, H. A. Stern, B. J. Berne, *J. Phys. Chem. B* **2002**, *106*, 12017.
[13] M. L. Sánchez, M. A. Aguilar, F. J. Olivares del Valle, *J. Comput. Chem*. **1997**, *18*, 313.
[14] M. L. Sánchez, M. E. Martín, M. A. Aguilar, F. J. Olivares del Valle, *J. Comput. Chem*. **2000**, *21*, 705.
[15] I. Fdez. Galván, M. L. Sánchez, M. E. Martín, F. J. Olivares del Valle, M. A. Aguilar, *Comput. Phys. Commun*. **2003**, *155*, 244.
[16] M. L. Sánchez, M. E. Martín, I. Fdez. Galván, F. J. Olivares del Valle, M. A. Aguilar, *J. Phys. Chem. B* **2002**, *106*, 4813.
[17] M. A. Aguilar, M. L. Sánchez, M. E. Martín, I. Fdez. Galván, In Continuum Solvation Models in Chemical Physics, 1st ed.; B. Mennucci, R. Cammi, Eds.; Wiley: New York, **2007**; Chapter 4.5, pp. 580–592.
[18] O. Tapia, In Theoretical Models Of Chemical Bonding; Z. B. MakSic, Ed.; Springer: Berlin, **1991**; Chapter 11, p. 435.
[19] J. G. Ángyán, *J. Math. Chem*. **1992**, *10*, 93.
[20] N. Okuyama-Yoshida, M. Nagaoka, T. Yamabe, *Int. J. Quantum Chem*. **1998**, *70*, 95.
[21] N. Okuyama-Yoshida, K. Kataoka, M. Nagaoka, T. Yamabe, *J. Chem. Phys*. **2000**, *113*, 3519.
[22] H. Hirao, Y. Nagae, M. Nagaoka, *Chem. Phys. Lett*. **2001**, *348*, 350.
[23] I. Fdez. Galván, M. L. Sánchez, M. E. Martín, F. J. Olivares del Valle, M. A. Aguilar, *J. Chem. Phys*. **2003**, *118*, 255.
[24] J. Simons, P. Jorgensen, H. Taylor, J. Ozment, *J. Phys. Chem*. **1983**, *87*, 2745.
[25] M. J. Frisch, G. W. Trucks, H. B. Schlegel, G. E. Scuseria, M. A. Robb, J. R. Cheeseman, V. G. Zakrzewski, J. A. Montgomery, Jr., R. E. Stratmann, J. C. Burant, S. Dapprich, J. M. Millam, A. D. Daniels, K. N. Kudin, M. C. Strain, O. Farkas, J. Tomasi, V. Barone, M. Cossi, R. Cammi, B. Mennucci, C. Pomelli, C. Adamo, S. Clifford, J. Ochterski, G. A. Petersson, P. Y. Ayala, Q. Cui, K. Morokuma, D. K. Malick, A. D. Rabuck, K. Raghavachari, J. B. Foresman, J. Cioslowski, J. V. Ortiz, A. G. Baboul, B. B. Stefanov, G. Liu, A. Liashenko, P. Piskorz, I. Komaromi, R. Gomperts, R. L. Martin, D. J. Fox, T. Keith, M. A. Al-Laham, C. Y. Peng, A. Nanayakkara, C. Gonzalez, M. Challacombe, P. M. W. Gill, B. Johnson, W. Chen, M. W. Wong, J. L. Andres, C. Gonzalez, M. Head-Gordon, E. S. Replogle, J. A. Pople, Gaussian, 98; Gaussian Inc.: Pittsburgh, **1998**.
[26] K. Refson, *Comput. Phys. Commun*. **2000**, *126*, 310.
[27] (a) A. D. Becke, *Phys. Rev. A* **1988**, *38*, 3098; (b) C. Lee, W. Yang, R. G. Parr, *Phys. Rev. B* **1988**, *37*, 785.
[28] Z. Liu, S. Huang, W. Wang, *J. Phys. Chem. B* **2004**, *108*, 12978.
[29] C. M. Breneman, K. B. Wiberg, *J. Comput. Chem*. **1990**, *11*, 361.
[30] P. Ewald, *Ann. Phys*. **1921**, *369*, 253.
[31] W. G. Hoover, *Phys. Rev. A* **1985**, *31*, 1695.
[32] E. Choi, J. McDaniel, J. R. Schmidt, A. Yethiraj, *J. Phys. Chem. Lett*. **2014**, *5*, 2670.
[33] C. J. Johnson, J. A. Fournier, C. T. Wolke, M. A. Johnson, *J. Chem. Phys*. **2013**, *139*, 224305.
[34] K. Matsumoto, R. Hagiwara, Z. Mazej, P. Benkič, B. Žemva, *Solid State Sci*. **2006**, *8*, 1250.
[35] A. R. Choudhury, N. Winterton, A. Steiner, A. I. Cooper, K. A. Johnson, *J. Am. Chem. Soc*. **2005**, *127*, 16792.
[36] G. Raabe, J. Köhler, *J. Chem. Phys*. **2008**, *128*, 154509.

Received: 16 March 2015
Revised: 9 June 2015
Accepted: 23 June 2015
Published online on 24 July 2015